

## Critical proof load for proof load testing of concrete bridges based on scripted FEM analysis

Chen, X.; Yang, Y.; Evangeliou, P.; Van Der Ham, H.

**Publication date**

2019

**Document Version**

Accepted author manuscript

**Published in**

Life-Cycle Analysis and Assessment in Civil Engineering

**Citation (APA)**

Chen, X., Yang, Y., Evangeliou, P., & Van Der Ham, H. (2019). Critical proof load for proof load testing of concrete bridges based on scripted FEM analysis. In D. M. Frangopol, R. Caspeele, & L. Taerwe (Eds.), *Life-Cycle Analysis and Assessment in Civil Engineering: Towards an Integrated Vision - Proceedings of the 6th International Symposium on Life-Cycle Civil Engineering, IALCCE 2018* (pp. 99-105). CRC Press / Balkema - Taylor & Francis Group.

**Important note**

To cite this publication, please use the final published version (if applicable). Please check the document version above.

**Copyright**

Other than for strictly personal use, it is not permitted to download, forward or distribute the text or part of it, without the consent of the author(s) and/or copyright holder(s), unless the work is under an open content license such as Creative Commons.

**Takedown policy**

Please contact us and provide details if you believe this document breaches copyrights. We will remove access to the work immediately and investigate your claim.

# Critical Proof Load for Proof Load Testing of Concrete Bridges based on Scripted FEM Analysis

Xin Chen & Yuguang Yang

*Faculty of Civil Engineering and Geosciences*

*Delft University of Technology, Delft, The Netherlands.*

Panagiotis Evangeliou

*DIANA FEA BV, Delft, The Netherlands.*

Herbert van der Ham

*Rijkswaterstaat, Utrecht, The Netherlands.*

**ABSTRACT:** As the bridge stock in The Netherlands and Europe is ageing, various methods to analyse the capacity of existing bridges are being studied. Proof load testing is one of the method to test the capacity of bridges by applying loads on the existing concrete bridges with small spans. Because of the fact that neither the actual traffic load nor the design traffic load required by Eurocode can be directly applied on the target bridge in real-life proof load testing, an equivalent wheel load has to be applied instead. The magnitude and the location of the equivalent wheel load is determined in such a way that it generates the same magnitude of inner forces in the cross section. Such calculation is usually done by linear finite element analyses (FEA). Whereas, different bridges have different geometry such as length, width, thickness, skewness, number of spans and lanes etc. For each configuration, FEA has to be done first to determine the loading position. The main aim of this paper is to study the relation between bridge geometry and unfavourable loading positions. Based on that, a guidance tool is developed for the determination of the critical proof load testing locations for the practice. To achieve this goal, a Python script has been developed using the general purpose FEM platform DIANA FEA. The script enables the automatic generation and analysis of a bridge model with different geometries and loading conditions. By applying the Eurocode Load Model 1 (LM1) at variable locations, the most unfavourable loading positions for the proof load are obtained at the corresponding boundary conditions. The output of the study provides a convenient tool for future proof load testing.

## 1 INTRODUCTION

In the Netherlands, many existing bridges are ageing and require detailed inspection. This is because of the high building activity in road and railway construction that occurred during the Post-World War II period, the fifties and sixties. Bridges built in this period are reaching their originally advised service life. Also, with the development of the society, both the number and the weight of the vehicles are increasing. Therefore, increasing requirement on assessment of the capacity and the remaining life time of existing bridges can be expected in the coming years.

Field testing can be used for instance when the effect of deterioration on the structural capacity is unknown. Proof load testing is one of the field test method that can assess the capacity of the structure. The common and widely accepted proof load testing

consists two stages, preparation stage and execution stage. One of the main tasks in the preparation stage is determining the critical proof load, which can be separated into two steps. They are: 1) to determine the location of the critical proof load. 2) to estimate the magnitude of the critical proof load that need to be applied during the test. The magnitude of the load should be able to sufficiently represent the appropriate safety level without causing any irreversible damages or the collapse of the structure.

In the Netherlands, proof load testing is often applied on the small span concrete slab bridges. In a concrete slab bridge, the determination of the critical proof load requires the moment and shear force calculation, which is not always straightforward. An accurate estimation usually requires finite element modelling. In this paper, a scripted FEM modelling tool is

provided to automatically determine the target magnitude and location of the critical proof load based on the design loading conditions. Simplified formulas for calculating critical proof load are obtained, which provides a convenient tool for the future proof load testing.

The focus of this paper is to proof loading the bending capacity of concrete slab bridges. For the shear capacity, a different approach has to be considered. The critical shear loading position of concrete slab bridges were studied in (Lantsoght, E. O. L. 2013)

## 2 SIMPLIFIED LOAD MODEL 1 (SLM1)

The loading configuration used in finite element model is based on LM1 (EN1991-2. 2011). As demonstrated in this paper, the same approach can be extended to other definition of loading conditions.

LM1 consists of two partial systems: tandem system and UDL (Uniformly Distributed Load) system. The tandem system contains double-axle concentrated loads, representing heavy lorries, should be placed at the most unfavourable location. UDL system consists of uniformly distributed load, representing the traffic flow, applied on the notional lanes and the remaining area.

In a proof load testing, the application of the load model is usually simplified by having only the tandem load, and it is defined as Simplified Load Model 1 (SLM1) in this paper.

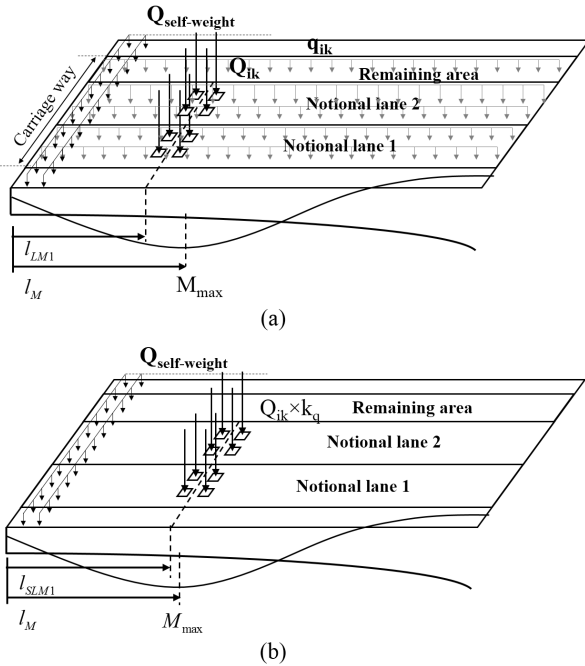


Figure 1: A comparison between the Eurocode Load model 1 (a) and the Simplified Load Model 1 (b).

Figure 1 (a), (b) shows the loading configuration of LM1 and the SLM1 respectively. The absence of UDL in the SLM1 will result in different inner forces distribution comparing with the original LM1. In order to

make the SLM1 generate the same magnitude of moment at the same critical cross section as the original LM1. The magnitude and position of the tandem load has to be adjusted.

In the SLM1, two factors  $k_q$  and  $k_p$  are introduced for tandem system. Factor  $k_q$  is named as the equivalent loading factor, which is responsible for the magnitude of the load. The tandem load specified in LM1 multiplied by  $k_q$  is the magnitude of tandem load that should be applied in the SLM1. Factor  $k_p$  is the critical position factor, which is a ratio between  $l_{SLM1}$  and the span length as shown in Figure 1 (b), where  $l_{SLM1}$  is the distance between the edge of the span and the middle of tandem system. The two factors  $k_q$  and  $k_p$  should be determined by comparing the inner force at the critical cross section of a specific target limit state. In the case of bridge, that is  $M_{max}$  when the tandem load is at the most unfavourable position.

To search for the maximum bending moment  $M_{max}$ , tandem system is moved from one end of the bridge deck to the other end along the nominate lane of the bridge with an increment of  $\Delta l$ . For each location,  $M_i$  can be found which represents the maximum bending moment of that tandem location. With the movement of tandem system, a series of maximum bending moment  $M_i$  of each loading location will be found:  $M_1, M_2, M_3 \dots M_n$ ,  $n$  is the total number of the cases of different locations. Then, it can be defined that:  $M_{max} = \max\{M_1, M_2, M_3 \dots M_n\}$ .  $M_{max}$  is the maximum bending moment represents the largest bending moment that can be possibly induced when tandem system moves through the entire span.

## 3 FINITE ELEMENT MODEL

### 3.1 Reference case: De Beek viaduct

The presented study selected a typical concrete slab bridge to create its baseline of the finite element model. The selected bridge is the De Beek viaduct, as it was previously proof loaded by Delft University of Technology in 2015 (Koekkoek, R. T. 2016). Then, skewness, span length, span width, average thickness and thickness ratio are parameterized to study their influence on the critical proof load.

De Beek is a 4-span concrete reinforced viaduct located over the highway A67 in Netherlands, as shown in Figure 2. It was constructed in 1963 and is owned and managed by Rijkswaterstaat, the Ministry of Infrastructure and Water Management. In this section, the dimension of this viaduct is illustrated.

In Figure 3 the top view of the first two spans of the viaduct is presented. The total width of the viaduct is 9940 mm and the width of the carriage way is 7440 mm. Cross section C-C' gives an overview of the thickness distribution over the length of the viaduct. It can be seen that the thickness of the slab in span 1 changes from 470 mm at the end support to 870 mm



Figure 2: Location of viaduct De Beek

at the intermediate support. The thickness of the slab in span 2 changes from 870 mm at the supports to 470 mm in the middle of the span. The end support beams has an additional thickness of 200 mm resulting in a total thickness of 670 mm. For the intermediate beams, the thickness increases with respect to the adjacent slab thickness is 250 mm which results a thickness of 1120 mm in total.

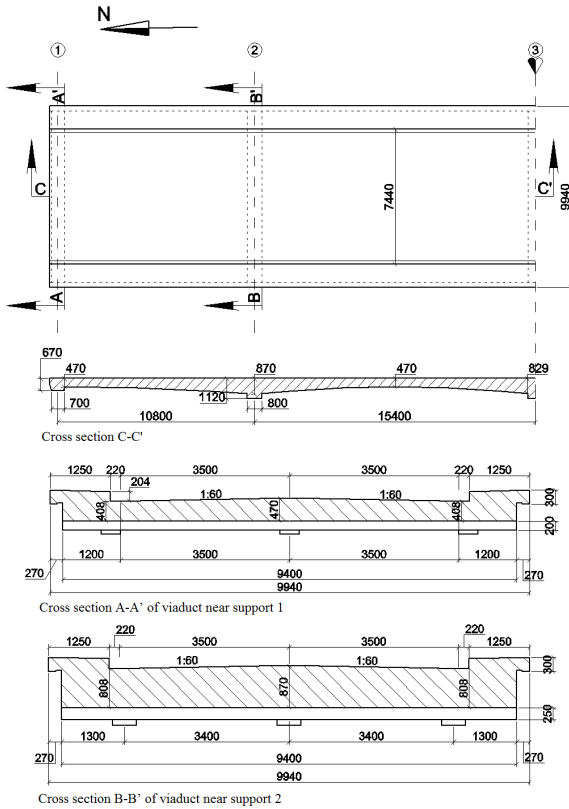


Figure 3: Dimensions of viaduct De Beek

The thickness of the viaduct also changes in the transverse direction. At the edges of the viaduct a kerb is present with a height of 200 mm. The height of the viaduct deck changes from 470 mm in the centre to 408 mm at the sides for the cross section near support 1 and from 870 mm at the centre to 808 mm at the side for the cross section near support 2. A layer of asphalt varying between 50 mm and 75 mm is present, according to the inspection report. (Koekkoek, R. T. 2016).

De beek is a 4-span bridge, but span 2 and span 3 are right above the highway A67. For safety reason,

it was decided that to perform proof load test on the span 1 only. Figure 4 illustrates the configuration of De Beek viaduct. Supports are simplified into point supports. Figure 5 shows the corresponding finite element model with a mesh size of 100 mm.

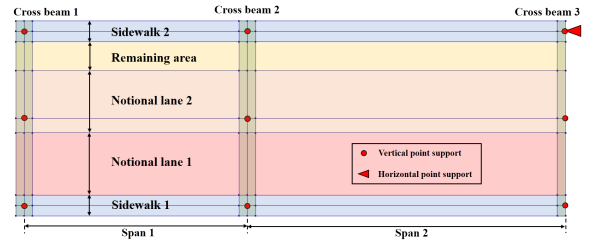


Figure 4: Configuration of De Beek viaduct

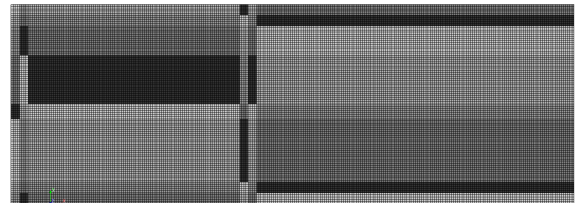


Figure 5: Finite element model with mesh size of 100mm

### 3.2 Geometry of deck slabs

Based on the study of the De Beek viaduct, the description of the geometry of slab bridge can be generalized. Skewness, span length, span width, average thickness and thickness ratio are studied to investigate their influences on critical proof load. The geometrical parameters used in this paper is illustrated in Figure 6.

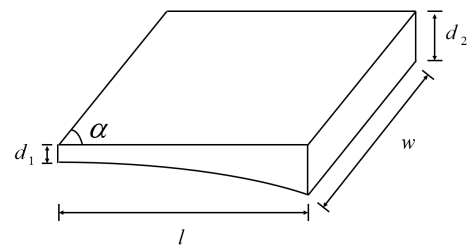


Figure 6: Geometrical parameters used in this paper

Where,

- $l$  is the length of tested span. Unit: meter [m].
- $w$  is the length of tested span. Unit: meter [m].
- $\alpha$  is the angle of skewness. Unit: degree  $^{\circ}$ .
- $d_1$  is the minimum thickness. Unit: meter [m].
- $d_2$  is the maximum thickness. Unit: meter [m].
- $r$  is the thickness ratio,  $r = d_2/d_1$ .

The thickness distribution along the span is simplified into circular shape. Thickness function has been

used to assign the thickness for the 2D deck. A thickness field need to be defined by the thickness function and the filed can be larger than the geometry shape of the deck. Figure7 shows the thickness field of the first span of De Beek viaduct and its boundary.

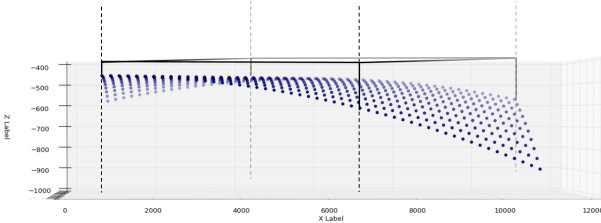


Figure 7: Thickness field of span1 and its boundary

### 3.3 Tandem System

The load of tandem system is simulated with quadrilateral force load in the finite element software DIANA. A quadrilateral force load defines a force that is distributed through a quadrilateral surface on a larger surface of 2D elements. The quadrilateral area is rectangular and the edges do not have to match with the element edges. Internally, the quadrilateral force load is converted to element surface load. The sum of forces and moments will be exactly matching with the user defined force value and position of the quadrilateral force load.(Manie J. and Kikstra M.P. 2017) For instance, in Figure 8, here it is seen that in P1 phase, there is no overlap between the loaded surface and the interest area, which means there will be no load applied on the interest area. In P2 phase, half of the loaded surface where indicated with shadow are overlapped with interest area. Thus, half of the load are applied on interest area. According to the same mechanism, all the load is applied on interest area in P3 phase.

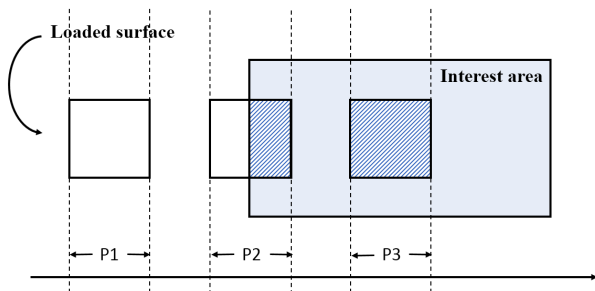


Figure 8: Mechanism of quadrilateral force

According to LM1, the loaded surface has an area of  $0.4 \text{ m} \times 0.4 \text{ m}$ , which represents the contact area between the wheel and the bridge surface. The compressive forces spread with an angle of  $45^\circ$ . In the 2D model, an equivalent tandem area is applied, which is the area that compressive force distributed on the middle layer of the bridge deck. Figure 9 shows the case when the thickness of asphalt and deck are 75 mm and 470 mm respectively.

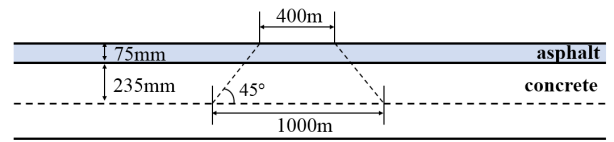


Figure 9: Equivalent tandem area

### 3.4 Post-process of bending moment

The results of the finite element analysis has to be further processed. In order to limit the mesh sensitivity and the thickness dependency of the bending moment. The probe curve are used to access the results. Probe curve is a fictitious curve that can be used to read the results from its surrounding integration points. As presented in Figure 10, two probe curves are set along the longitudinal and the transverse direction with a length of 1 meter. The intersection of the two probe curves is the location of the maximum bending moment  $M_{max}$ . Here to calculate the equivalent bending moment, the effect of the thickness of the slab is taken into account by assuming the internal level arm of the cross section that is linearly related to the slab thickness. The following steps described how  $M_{max}$  is processed using python script:

- (i) Search for the maximum bending moment within span 1 and its position.
- (ii) Create probe curve  $x$  (longitudinal direction) and probe curve  $y$  (transverse direction) with a length of 1 meter.  $M_{max}$  is located at the intersection of curve  $x$  and  $y$ .
- (iii) Extract the corresponding bending moment  $\{Mx\}_i$  and  $\{My\}_i$  of nodes  $px_i$  and  $py_i$ .
- (iv) Extract the corresponding thickness  $dx_i$ ,  $dx_i$  of points  $px_i$  and  $py_i$ .
- (v) Calculate  $\{Mx\}_i/dx_i$  and  $\{My\}_i/dy_i$ .
- (vi) Take the average of all the points as modified bending moment:  $M_{md,max} = (\sum_{i=1}^{11} \{Mx\}_i/dx_i + \{My\}_i/dy_i)/22$

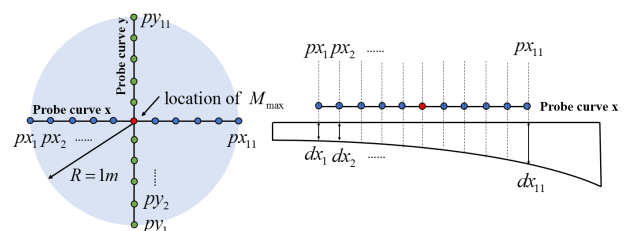


Figure 10: Use probe curve to access moment

Table 1: List of parameters

Parameters	ranges
Skewness	90°-60°
Span width	9m-13m
Span length	6m-15m
Average thickness	0.3m-1.3m
Thickness ratio	1.10-2.8

## 4 PARAMETRIC STUDY

Different input geometrical parameters, their influences on critical proof load are analysed with a large set of models created by Python scripts. A diagram shown in Figure 11 illustrates the flow of Python scripts. A model is created using the input geometrical parameters, and loaded based on LM1 to search for the  $M_{max}$ . Then, based on the obtained  $M_{max}$ , the output  $k_p$  and  $k_q$  can be find according to SLM1.

Using the data provided by Rijkswaterstaat. The ranges of the input parameters are selected in a way that most of the existing bridges and viaducts configurations in Netherlands are covered.

The five parameters have been divided into four groups, namely, the span length and thickness group, the thickness ratio group, the span width group and the skewness group. The span length and thickness group contains two parameters since they are not independent. Increasing the length leads to an increase of thickness, satisfying the following equation:  $(l_i/l_0)^2 = d_i/d_0$ , where  $l$  and  $d$  are the length and the thickness of a span respectively. The skewness group is combined with the span width group, the length and thickness group, and the thickness ratio group as shown in Figure 12.

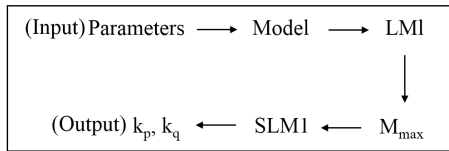


Figure 11: Flow diagram of Python scripts

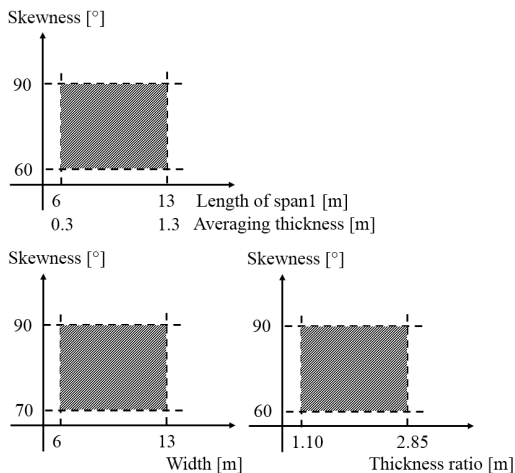


Figure 12: Visualization of combined parameters

## 5 RESULTS

Results are presented in two types of graphs, namely the critical position factor graph and the equivalent loading factor graph, corresponding to the two factors  $k_p$  and  $k_q$  as discussed in section 2.

### 5.1 Skewness

Figure 13 shows the relation between the critical position factor  $k_p$  and the angle of skewness  $\alpha$ . Here it is seen that with the decrease of the angle  $\alpha$ ,  $k_p$  increase from 0.36 to 0.56, which means the critical loading position moves away from the edge of the span to the middle. Trendline shows a linear relation between  $k_p$  and  $\alpha$ . Figure 14 described the linear relation between  $k_q$  and  $\alpha$ .

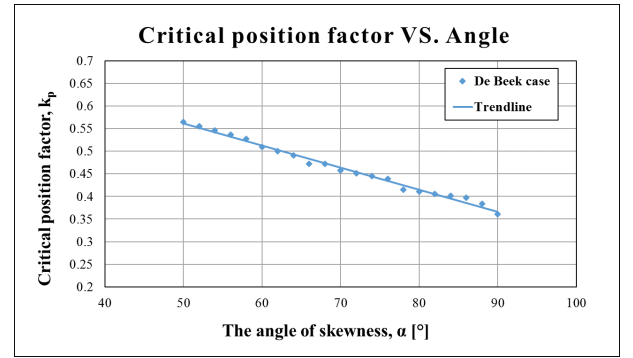


Figure 13: Critical position factor versus skewness

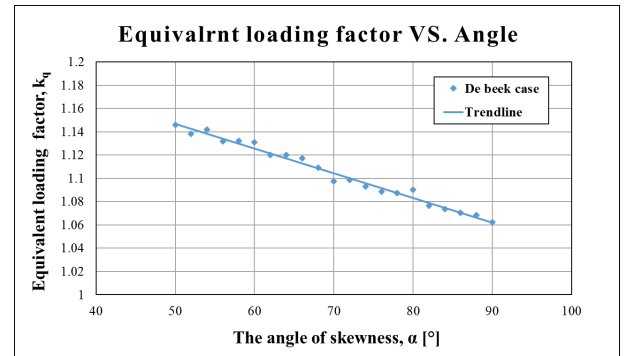


Figure 14: Equivalent loading factor versus skewness

### 5.2 Span Width

Figure 15 shows that  $k_p$  is independent to the variation of  $w$ . Attention need to be paid on the constant vertical intervals between the trendlines. The constant interval denotes that  $k_p$  increases with a constant rate when the angle  $\alpha$  drops, which is coincided with the trend shown in Figure 13.

In Figure 16, it is shown that in spite of a small slope, the effect of  $w$  to  $k_q$  is limited.



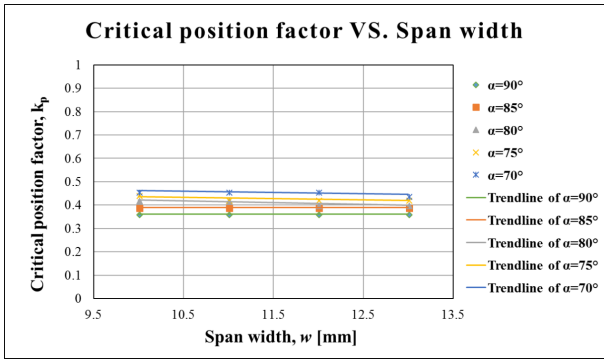


Figure 15: Critical position factor versus width

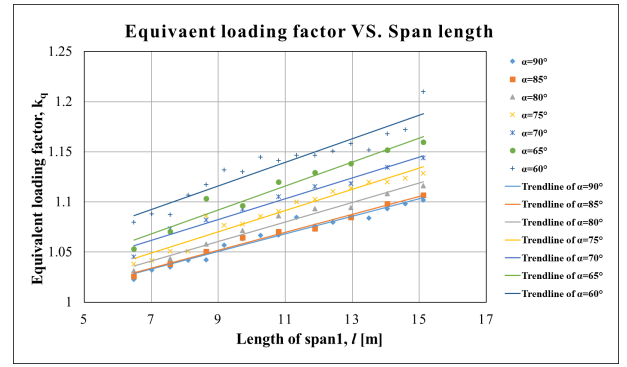


Figure 18: Equivalent loading factor versus span length

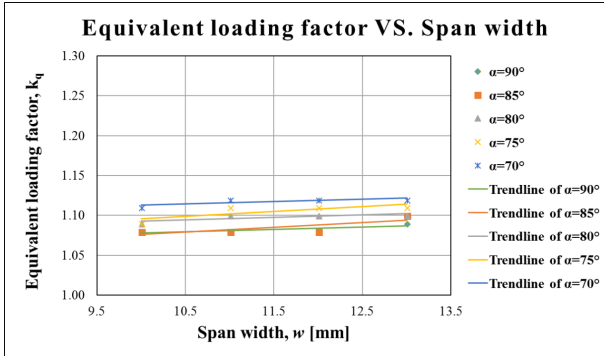


Figure 16: Equivalent loading factor versus width

### 5.3 Span Length and Thickness

In this group, the length of the span changes from 6.48 to 15.12 m and with a corresponding thickness changing from 0.17 to 0.92 m. Figure 17 shows the relation between  $k_p$  and  $l$ . Taking  $\alpha=90^\circ$  as an example,  $k_p$  decreases linearly with the increase of length  $l$ . However, the decreasing trend shown for all angle ranging from  $60^\circ$  to  $90^\circ$ , but the slopes are different. The intervals between different angle at  $l=6.58$  m is larger than intervals at  $l=15.12$  m. This means the span length  $l$  do not only affect the critical loading position, but also the relation between  $k_p$  and  $\alpha$ .

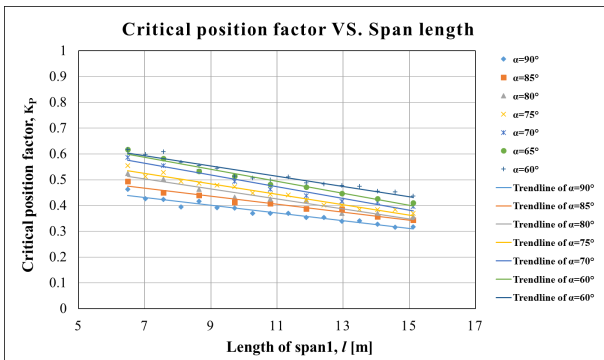


Figure 17: Critical position factor versus span length

Figure 18 presents the relation between  $k_q$  and  $l$ .  $k_q$  increases with the increase of  $l$ , and the trendlines seems to be linear. Whereas, it can also be observed that the intervals of the adjacent trendlines become larger with the decrease of angle  $\alpha$ .

### 5.4 Thickness ratio

Figure 19 shows the relation between the critical position factor  $k_p$  and the thickness ratio  $r$ . Here it is seen that the change of  $k_p$  based on  $r$  can be predicted by parabolic curves. When  $r$  is smaller than 2, there is a strong dependency between  $k_p$  and  $r$ . When  $r$  is between 2.35 and 2.85,  $k_p$  is not sensitive to  $r$  any more. The intervals between the different curves are the same, which means with the increase of  $\alpha$ , critical position factor decreases with a constant rate.

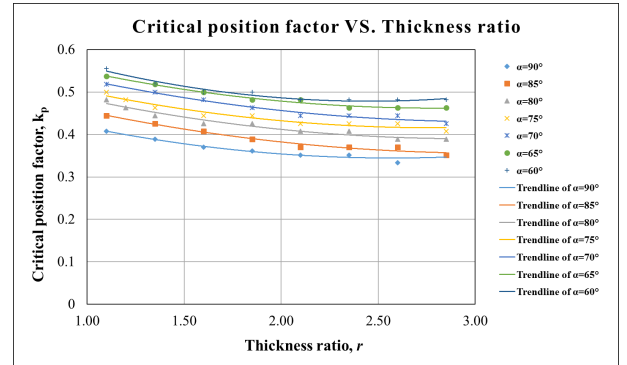


Figure 19: Critical position factor versus thickness ratio

The relation between the equivalent loading factor  $k_q$  and the  $r$  can be described by straight lines as shown in Figure 20.  $k_q$  decreases with the increase of  $r$ . However, the slopes of those lines are different. This means the sensitivity between  $k_q$  and  $r$  can be affected by the skewness.

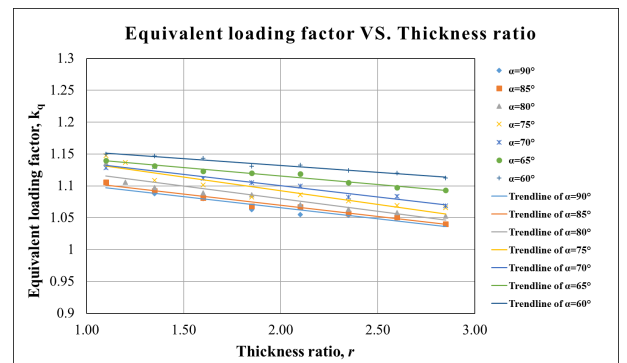


Figure 20: Equivalent loading factor versus thickness ratio

## 5.5 Extrapolation of the general formulas

As discussed in the previous sections,  $k_p$  and  $k_q$  can be affected by the span  $l$ , the thickness ratio  $r$ , and the skewness  $\alpha$ . Thus,  $k_p$  and  $k_q$  can be formulated as a function of  $l, r$  and  $\alpha$  respectively. By applying linear least squares regression with 166 sets of data obtained from the numerical results. Formulas of  $k_p$  and  $k_q$  are obtained:

$$k_p = 0.002lr^2 - 0.0123lr - 0.000038l\alpha - 0.0043\alpha + 0.9684$$
$$k_q = 0.0055lr - 0.0012r\alpha + 0.000043\alpha + 1.1518$$

A comparison has been made between the numerical results and the predicting results calculated using the above formulas. For  $k_p$ , among all the 166 points, the maximum relative error is 8.8% and the mean relative error is 2.1%. For  $k_q$ , the maximum relative error is 3.1% and the mean relative error is 0.59%. These expressions of  $k_p$  and  $k_q$  were determined based on LM1. For bridges which has to be assessed by different load models according to different codes, the formulas have to be recalibrated.

## 5.6 Sensitivity of $k_p$ and $k_q$

For the critical position factor  $k_p$ , applying the critical proof load at the predicted position with an allowable error of  $\pm 0.5m$  will lead to a maximum error of 2% for bending moment. For the equivalent loading factor  $k_q$ , the relation between  $k_q$  and the bending moment is linear. However, the accuracy of the simplified expression is relatively high.

## 6 CONCLUSION AND RECOMMENDATIONS

Bridges with different geometrical configurations have been studied with linear finite element analysis. The aim is to find the magnitude and location of the critical proof load to simplify the loading condition. Five different parameters, namely skewness, span length, span width, average thickness and thickness ratio, are studied to investigate their influence on critical proof load are found. In total, 166 sets of data are obtained by performing thousands of finite element analyses. Formulas for predicting critical position factor  $k_p$  and equivalent loading factor  $k_q$  are proposed by these data and they are approved to be capable enough to predict the results.

The possible improvements of the presented study are discussed below. Most of them can be achieved by directly modifying the python script.

According to LM1, EC1991-2. The increase of width may lead to the increase of notional lanes, which is not included in this paper. Further analysis is needed to search the influence of extra notional lanes on critical proof load.

The equivalent critical proof load was found by applying two sets of tandem systems. However, in real-

ity the second tandem system is not always possible. The equivalent critical proof load of one tandem system should be applied in this case.

In this paper,  $k_p$  and  $k_q$  of other safety levels can be obtained by changing the design load in python script. In order to maintain the same safety level, the target limit state should be estimated taking into account the original uncertainty of the design load and the resistance of the structure when it was designed. In (Casas and Gmez 2013) (Val and Stewart 2002) such analysis is demonstrated.

The thickness distribution has been simplified into circular curve. Whereas, the thickness distribution is more complicated in reality, it is considered necessary to describe the thickness in a more accurate way since the bending moment is very sensitive to thickness.

The parameters that analysed in this paper is span length, width, skewness and thickness ratio, however, more parameters can be included, such as the number of spans, the length ratio between different span etc.

## REFERENCES

- Lantsoght, E. O. L., van der Veen, C., de Boer, A. & Walraven, J. C. (2013). Recommendations for the Shear Assessment of Reinforced Concrete Slab Bridges from Experiments, Structural Engineering International, V. 23, No. 4, pp. 418-426.
- EN1991-2.,(2011). Eurocode 1: Actions on structures Part 2: Traffic loads on bridges.
- Koekkoek, R. T., Lantsoght, E. O. L., Yang, Y. & Hordijk, D. A. (2016). Analysis Report for the Assessment of Viaduct De Beek by Proof Loading, Stevin Report 25.5-16-01, Delft University of Technology, Delft, the Netherlands, 125 pp.
- Manie J.& Kikstra W.P. (2017). DIANA User's Manual, 10.2, Ed.
- Casas, J. R.& Gmez, J. D. (2013). Load Rating of Highway Bridges by Proof-loading, KSCE Journal of Civil Engineering, V. 17, No. 3, pp. 556-567.
- Val, D. & Stewart, M. G. (2002). Safety factors for assessment of existing structures. J StructEng, ASCE 2002;128(2):25865.